ACS APPLIED MATERIALS & INTERFACES

Research Article

www.acsami.org

# Effect of Fluorination on Electronic Properties of Polythienothiophene-*co*-benzodithiophenes and Their Fullerene Complexes

Ram S. Bhatta* and Mesfin Tsige*

Department of Polymer Science, The University of Akron, Akron, Ohio 44325, United States

**ABSTRACT:** Fluorination of conjugated polymers is a popular way of designing new electron donors for the bulk heterojunction (BHJ) based organic solar cells (OSCs). However, not all fluorinated polymers observed experimentally enhance the power conversion efficiency of OSCs, and the fundamental understanding of the effect of fluorination is not yet fully uncovered. Herein, we report the effect of fluorine substitution on the electronic properties of polythienothiophene-*co*-benzodithiophenes as well as their complexes with fullerene, using density functional theory (DFT) and time-dependent DFT methods at the molecular level. Systematic computations of energy gaps ($E_g^{opt}$ and $E_g^{hl}$), ionization potentials (IP), electron affinities (EA), molecular electrostatic potential (MEP) surfaces, and dipole moments ($\mu$) are carried out for these systems. We found that the fluorination of the thienothiophene unit favors lower $E_g^{opt}$, $E_g^{hl}$, IP, and EA as well as stronger $\mu$ compared to the fluorination of the benzodithiophene unit, suggesting that efficient exciton dissociation and charge carriers formation may take place efficiently for the former case. These results support recent experimental findings that the performance of polythienothiophene-*co*-benzodithiophene-based organic solar cells enhances when thienothiophene unit is fluorinated. The present results highlight that more efficient conjugated polymers for OSC can be designed if the gap engineering is carried out by focusing on the low IP, low EA, and high dipole moment.

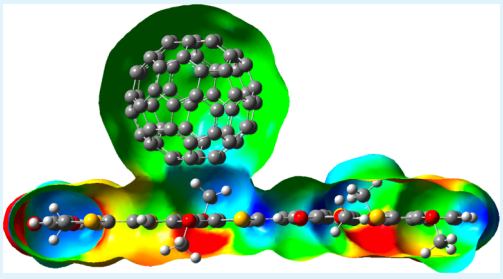

**KEYWORDS:** *first-principles calculations, fluorinated copolymers, organic solar cell, band gap, dipole moment, molecular electrostatic potential surface*

## 1. INTRODUCTION

Bulk heterojunction (BHJ)-based organic solar cells (OSCs) are promising candidates for clean, renewable and sustainable energy because of their flexibility, lightweight, ease of processing, low cost, low potential for adverse environmental impact and high carrier mobility.[1−9] The current power conversion efficiency (PCE) of BHJ based OSCs has reached ∼9.2%.[10] However, the performance of these devices needs to be further enhanced for their successful commercialization and practical realization. BHJ-based OSCs are complex systems in which organic conjugated polymers (electron donors) are blended with fullerene derivatives (electron acceptors).[11,12] Performance of such devices depends on various factors: the most important of these are the valence-to-conduction band gaps (energy gaps) of the conjugated polymers, the BHJ morphology and the distribution of components at interfaces.[13−17] These factors are directly or indirectly associated with the chemical structures of the conjugated polymers because a slight modification in the chemical structure alters the molecular orbital energies, which in turn affect the electronic properties and intramolecular and intermolecular interactions.[16,18,19] Therefore, structural modification and designing of high performing conjugated polymers with improved electronic properties are crucial to enhance the performance of OSCs.

Several experimental studies[16,20−28] on structural modification of polymers have revealed that the performance of polymers can be tuned by introducing the electron-withdrawing fluorine atom to the polymer backbone. Among the fluorinated polymers, the partially fluorinated derivative of polythienothiophene-*co*-benzodithiophene (PTB2) (PTB7 in Figure 1) is the current champion used in OSCs.[10] Interestingly, not all the fluorinated derivatives of PTB2 enhance the PCE of OSCs. For instance, the fluorination of thienothiophene unit increases, whereas the fluorination of benzodithiophene unit as well as the perfluorination of PTB2 decrease the PCE of OSC.[16] Although the synthesis and the performance of fluorinated derivatives of PTB2 on OSCs are studied experimentally, fundamental reasons behind their variable performances from the first-principles study remain unexplored. This requires the investigation of fundamental properties such as molecular electrostatic potential, electron affinity, ionization potential, dipole moments, and donor/acceptor interactions at the molecular level, which is the focus of the present study. Understanding of these fundamental properties is crucial for the structural modification and designing of efficient polymers for further enhancing the PCE of OSCs.

**Received:** June 3, 2014
**Accepted:** August 26, 2014
**Published:** August 26, 2014

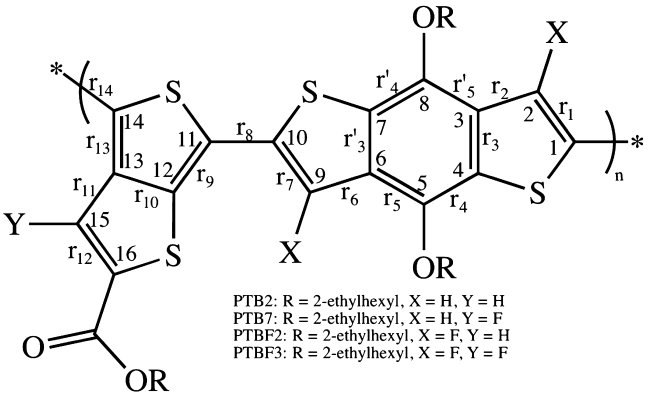


**Figure 1.** Schematic representation of polythienothiophene-*co*-benzodithiophene and its fluorinated derivatives.

In this work, we perform systematic first principle calculations to investigate the effect of fluorination on the electronic properties of polythienothiophene-*co*-benzodithiophenes and their fullerene complexes. We compute energy gaps, electron affinity, ionization potential, molecular electrostatic potential, dipole moment and interactions of fluorinated derivatives of PTB2 with fullerene at the molecular level. We discuss implications of the present results in designing efficient conjugated polymers for BHJ-based OSCs.

## 2. COMPUTATIONAL METHODS

Our recent studies[29,30] have shown that Becke's three−parameter Lee−Yang−Parr exchange-correlation functional (B3LYP)[31] upon dispersion correction using Grimme approach[32] produces accurate structural and electronic properties of PTB7. The B3LYP functional is also well-known to produce accurate structural and electronic properties of similar conjugated polymers.[33−38] In the present study, we follow our previous approaches[29,30] to fully optimize ground state geometries of PTB2, PTB7, PTBF2 and PTBF3 oligomers up to the pentamer using B3LYP/3-21G* followed by the ground and the excited state computations at B3LYP/6-31G*. All density functional theory (DFT)[39] and time-dependent density functional theory (TDDFT)[40] calculations were performed using NWChem 6.1[41] and Gaussian 09[42] packages.

From ground state calculations, HOMO−LUMO gap of each oligomer of PTB2, PTB7, PTBF2 and PTBF3 was calculated as the difference between HOMO and LUMO energies. The vertical excitation energies (optical gaps) from the ground state ($S_0$) to the first excited stete ($S_1$) were calculated for these oligomers using TDDFT. Both computed HOMO−LUMO and optical gaps for finite oligomers were then extrapolated to the polymer limit using Kuhn extrapolation technique.[43,44] The ionization potential (IP) and electron affinity (EA) were calculated from the total energies of neutral and charged oligomers as,

$$\mathrm{EA} = E(0) - E(-1) \quad (1)$$

$$\mathrm{IP} = E(+1) - E(0) \quad (2)$$

Here, $E(0)$, $E(-1)$ ,and $E(+1)$ are total energies of neutral, negatively charged and positively charged oligomers, respectively. To investigate the electronic properties of oligomer/fullerene complexes, each of the oligomer and fullerene was initially optimized separately. The oligomer/fullerene complexes were then constructed by positioning the fullerene close to the central benzodithiophene of the backbone. Each of these complexes was optimized at constrained donor−acceptor distances to calculate minimum-energy complexes and their electronic properties.

## 3. RESULTS AND DISCUSSION

**3.1. Isolated Oligomers.** *3.1.1. MEP and BLA.* We start with the computed results on isolated PTB2, PTB7, PTBF2, and PTBF3 oligomers. Fluorine is an electronegative atom and hence it exhibits inductive effect by pulling the electron density toward it when bonded with a carbon atom of the backbone. The changes in the electron density across the oligomers as a result of inductive effect of the fluorine atom can be visualized from the three-dimensional molecular electrostatic potential (MEP) surfaces (Figure 2a). The distribution of positive and

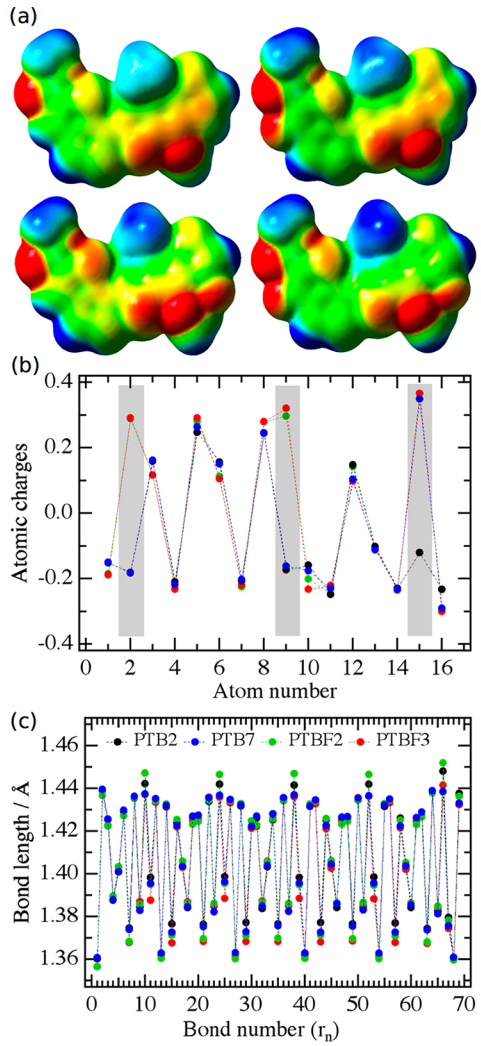


**Figure 2.** Effect of fluorination on (a) MEP, (b) Mulliken atomic charges, and (c) bond length of polythienothiophene-*co*-benzodithiophene derivetives. In a, PTB2, PTB7, PTBF2, and PTBF3 are top left, top right, bottom left, and bottom right, respectively. Refer to Figure 1 for the definition of atom and bond numbers. Dotted lines are guides for the eyes.

negative charges within the MEP surfaces of PTB2, PTB7, PTBF2 and PTBF3 are depicted by blue and red colors, respectively. In Figure 2a, the intense red color in PTB2 corresponds to oxygen atoms and the area covered by red color increases in the order PTB2 < PTB7 < PTBF2 < PTBF3 because of the increasing composition of fluorine atoms. As a result of change in electron densities in MEP surfaces upon fluorination, the atomic charges vary as shown in Figure 2b. Although the absolute magnitude of Mulliken atomic charges

depends on the size of the basis sets, the change of Mulliken atomic charges as a function of structural modification provides chemically meaningful insight even with the minimal basis sets.[45] As can be seen in Figure 2b, relative atomic charges of $C_2$, $C_9$, and $C_{15}$ (highlighted with shadow-bars) change not only in magnitude, but also in sign, drastically upon fluorination.

The change in the electron density also affects the bond length alterations (BLAs) in PTB2, PTB7, PTBF2 and PTBF3 because the bond between atoms within these polymers is formed by sharing the electron density. Figure 2c shows the change in BLAs for PTB2, PTB7, PTBF2 and PTBF3 pentamers. Atom and bond indices shown in Figure 2 are as defined in Figure 1. The electronegative fluorine atom exhibits an inductive effect thereby pulling electron density of the conjugated system toward it. Consequently, bond lengths in the neighborhood of fluorine atom are affected. The effect is noticeable for C−C single and double bonds that are adjacent to the C−F bond, with the change in bond length reaching as high as ∼0.01 Å (Figure 2c).

These changes in BLAs in PTB2, PTB7, PTBF2, and PTBF3 oligomers vary the intramolecular interactions, which in turn, affect the planarity of the backbone. In the present study, these structurally similar oligomers are found to have slightly different backbone nonplanarity. This increases with fluorine substitution and reaches a nonplanarity up to ∼30°. Son et al.[16] have reported the nonplanarity of the backbone in these oligomers up to ∼20° calculated at B3LYP/6-31G*. Our calculations with dispersion-corrected B3LYP show slightly increased nonplanarity, which is expected when including dispersion interactions. Our recent study[29] with dispersion-corrected B3LYP shows a nonplanarity of ∼25° in the PTB7 backbone.

*3.1.2. Energy Gaps.* The computed vertical excitation energies ($E_g^{opt}$) and HOMO−LUMO gaps ($E_g^{hl}$) of PTB2, PTB7, PTBF2, and PTBF3 are plotted in Figure 3. The

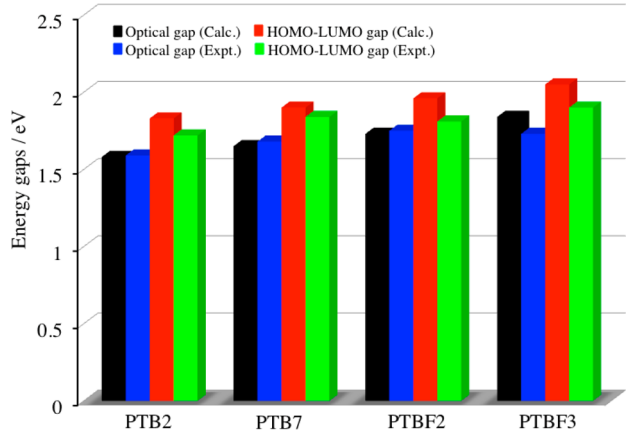


**Figure 3.** Effect of fluorination on energy gaps as shown. Experimental values of energy gaps are from ref 16

available experimental values of $E_g^{opt}$ and $E_g^{hl}$ determined from UV−vis absorption spectroscopy and cyclic voltametry, respectively,[16] are also included in Figure 3 for comparison. These experimental data are for long oligomer chains with $1/N \leq 0.005$, where N is the number of carbon−carbon double bonds along the shortest path through the backbone of chains. The computed $E_g^{opt}$and $E_g^{hl}$ are also estimated to the polymer limit (i.e., $1/N \approx 0$) to facilitate direct comparison between the computed and the experimental data. For this, $E_g^{opt}$ and $E_g^{hl}$ are calculated for oligomers up to the pentamer and are extrapolated to the long chain limit using Kuhn extrapolation technique.[43,44]

Both computed and experimental values of $E_g^{opt}$ and $E_g^{hl}$ increase with the substitution of fluorine atom to the thienothiophene and/or benzodithiophene units of oligomers. For instance, substitution of a fluorine atom to the thienothiophene unit increases the calculated values of $E_g^{opt}$ and $E_g^{hl}$ from 1.58 and 1.83 eV to 1.65 and 1.90 eV, respectively. The corresponding increases in the experimental values of $E_g^{opt}$ and $E_g^{hl}$ are from 1.59 and 1.72 eV to 1.68 and 1.84 eV, respectively.[16] Hence, the computed values show good agreement with the experimental results in terms of the relative increment of $E_g^{opt}$ and $E_g^{hl}$ upon fluorine substitution for all oligomers. However, the absolute values of computed energy gaps, particularly $E_g^{hl}$, are slightly overestimated compared to the experimental values. The small differences between computed and experimental energy gaps can be due to intermolecular and solvent effects that are present in the experimental measurements but not in the simulation.

*3.1.3. Electron Affinities and Ionization Potentials.* Ionization potentials (IP) and electron affinities (EA) are as important electronic properties as the energy gaps discussed above. The values of IP and EA determine the ease of ionization of PTB2 derivatives in the presence of the sunlight and efficient electron transfer to the fullerene molecule. In general, efficient electron transfer from the donor to the acceptor occurs if the former has lower IP and the later has higher EA. In other words, the relative IP of the donor and the EA of the acceptor determines the open-circuit voltage ($V_{oc}$), which is the crucial parameter of OSC devices. The higher the value of $V_{oc}$, the higher is the PCE of OSCs. Hence, among the fluorinated derivatives of PTB2, the one with the lowest IP and EA is expected to be the most efficient candidate.

The computed values of IP and EA for PTB2, PTB7, PTBF2, and PTBF3 oligomers up to the pentamer are summarized in Figure 4 as a function of $1/N$. Here, $N$ is the number of carbon−carbon double bonds along the shortest path through the backbone of each oligomer. Values of IP decrease (Figure 4a), whereas values of EA increase (Figure 4b) with the increase in polymer chain length for all the oligomers investigated in the present study. The variation in the values of IP and EA reaches up to ∼0.2 eV for perfluorinated oligomers compared to the unfluorinated oligomers (Figure 4). In general, effect of fluorination on IP and EA in the long-chain limit follows the order: PTB2 < PTB7 ≈ PTBF2 < PTBF3. To the best of our knowledge, there are no reported IP and EA values of these oligomers for the direct comparison of the present work. However, the nature of the variation of these values with $1/N$ (Figure 4) is similar to the reported values for polythiophene.[46]

**3.2. Fullerene/Polymer Complexes.** *3.2.1. Equilibrium Separation.* The donor−acceptor distance ($r_{D-A}$) of polymer/fullerene complex is one of the crucial parameters affecting the performance of OSCs because it controls the electron transfer process from the donor to the acceptor molecule. For the efficient intermolecular electron transfer, the donor and the acceptor molecules have to be spatially very close (≤4 Å) to promote significant overlap of electronic wave functions.[47,48] Hence, it is fundamentally important to investigate if there is any influence of fluorine substitution on $r_{D-A}$. For this, isolated fullerene, PTB2, PTB7, PTBF2 and PTBF3 oligomers were

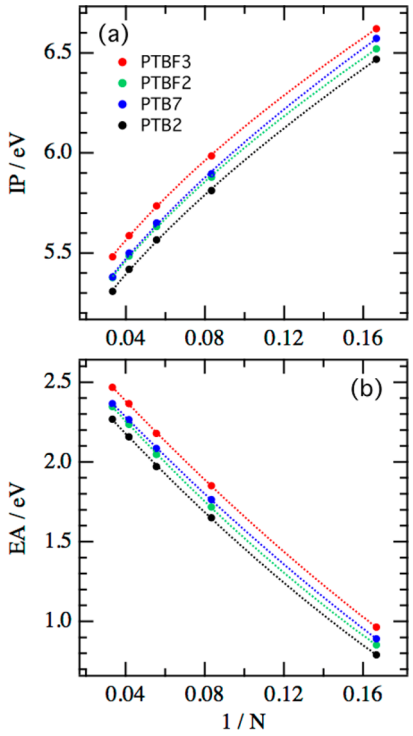


**Figure 4.** Variation of (a) IP and (b) EA as a function of the reciprocal of the number of C−C double bonds across the polymer backbone. Dotted lines are guide for the eyes.

initially optimized using dispersion corrected B3LYP without any constraint. The fullerene molecule was then placed through its hexagonal face close to the central hexagonal ring of PTB2, PTB7, PTBF2, and PTBF3 oligomers. These fullerene/oligomer complexes were then optimized at several constrained $r_{D-A}$.

Figure 5 shows the variation of total energies of polymer/fullerene complexes as a function of $r_{D-A}$. Plotted Energies in Figure 5 are relative to the minimum energy for each complex. The present study shows a minimum energy at $r_{D-A} \approx 3.5$ Å for all complexes of PTB2, PTB7, PTBF2 and PTBF3 with fullerene, suggesting that fluorination has negligible effect on $r_{D-A}$. Energies of complexes increase when $r_{D-A} > 3.5$ Å and

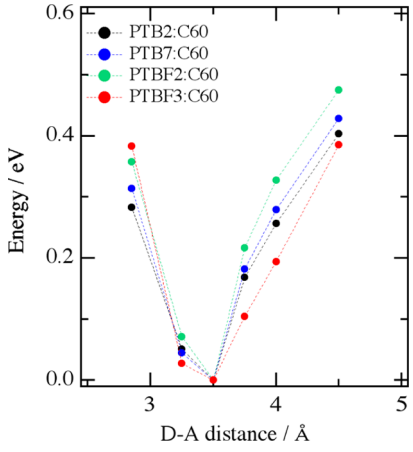


**Figure 5.** Relative total energies of fullerene/polymer complexes as a function of their separation distance. Dotted lines are guides for the eyes.

$r_{D-A} < 3.5$ Å, and follow the general order, $E_{C60/PTBF3} > E_{C60/PTBF2} > E_{C60/PTB7} > E_{C60/PTB2}$. Although there are no reported data for direct comparison of such variation of energies across $r_{D-A}$, the present results are supported by reported P3HT/fullerene results. Marchiori and Koehler[49] have found the minimum energy of P3HT/fullerene complex at $r_{D-A} \approx 3.5$ Å, consistent with the present study. In a practical OSC device, conjugated polymer chains are blended with fullerene molecules. The polymer chain conformations are controlled by intermolecular interactions, which in turn could be affected by fluorination. The donor−acceptor distance, which is connected with the accessibility of the polymer backbone to the fullerene molecule, could be slightly different from the equilibrium polymer/fullerene complexes in vacuum.

*3.2.2. Molecular Electrostatic Potential Surfaces.* Substitution of an electropositive hydrogen atom of a polymer backbone with an electronegative fluorine atom is expected to change the charge distributions of complexes. This can be better understood by creating molecular electrostatic potential (MEP) surfaces because they allow three-dimensional visualization of the different charged regions of complexes. Figure 6 shows the distribution of positive and negative charges within the complexes of fullerene with dimers of PTB2, PTB7, PTBF2, and PTBF3. In Figure 6, the blue color represents an area of low electron density and has a positive charge. On the other hand, areas of red color are characterized by an abundance of electrons and have negative charges. Hence, the spherical region of a complex that corresponds to electronegative fluorine and oxygen atoms has red color in Figure 6. Fluorine atoms are absent in fullerene/PTB2 complex and hence the intense-red color corresponds to oxygen atoms (Figure 5a). Fullerene/PTB7 (Figure 5b) and fullerene/PTBF2 (Figure 5c) complexes involve fluorinations of thienothiophene and benzodithiophene units, respectively, that are distinct from more extended red color compared to Figure 6a. Similarly, Figure 6d represents the extension of negative charge on both thienothiophene and benzodithiophene regions of the fullerene/PTBF3 complex.

An important feature evident from Figure 6 is that the fluorination increases electron density at the interface of fullerene and polymer. This affects the atomic charges on carbon atoms in fullerene, particularly atoms that are cofacial to the polymer backbone. This effect can be characterized quantitatively by calculating the atomic charges of carbon atoms in isolated fullerene and fullerene complexes. Figure 7 shows the change in atomic charges on carbon atoms of fullerene that are cofacial to the polymer backbone before and after the complex formation. The atomic charges vary from ∼0.02 au for fullerene/PTB2 to ∼0.05 au for fullerene/PTBF3 complexes. In general, the difference in charges before and after the complex formation increases with the fluorine substitution.

*3.2.3. Dipole Moment.* The computed ground state dipole moments of isolated PTB2, PTB7, PTBF2, and PTBF3 oligomers as well as their complexes with fullerene are summarized in Figure 8. The change in electron density upon fluorination causes the fluctuation in dipole moments across the isolated oligomers. Consequently, PTB2, PTB7, PTBF2, and PTBF3 dimers have dipole moments of 1.2, 4.13, 1.46, and 4.71 D, respectively. These results indicate that fluorination of the thienothiophene unit has pronounced effect on the dipole moments whereas fluorination of the benzodithiophene unit has negligible effect. Carsten et al.[50] have also observed the similar effect and have reported that the fluorination in the

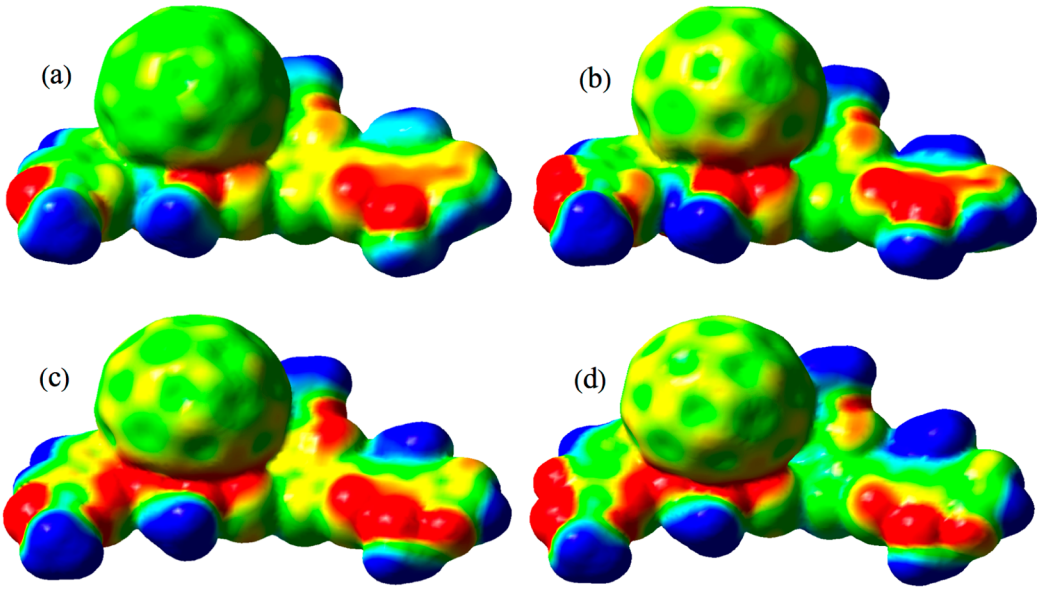


**Figure 6.** MEP surfaces of (a) fullerene/PTB2, (b) fullerene/PTB7, (c) fullerene/PTBF2, and (d) fullerene/PTBF3 complexes.

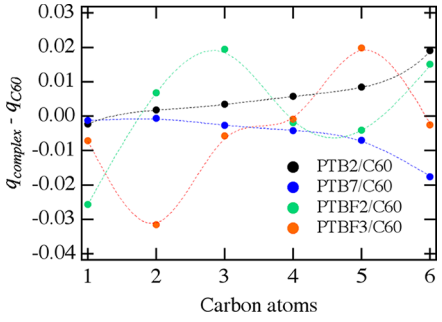


**Figure 7.** Variation in Mulliken charges on carbon atoms of fullerene that are cofacial to the polymer backbone during the complex formation. Dotted lines are guide for the eyes. See Figure 1 for the notation.

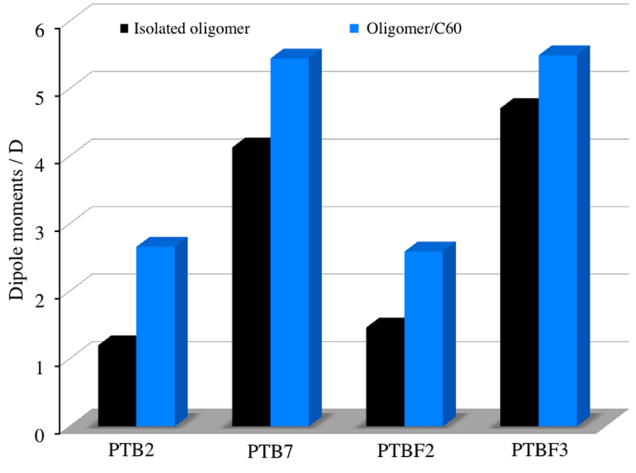


**Figure 8.** Computed ground-state dipole moments of isolated PTB2, PTB7, PTBF2, and PTBF3 dimers and their complexes with fullerene.

thienothiophene unit of PTB7 dimer results in the ground state dipole moment of 4.10 D, consistent with the present calculations. These results can be understood in terms of the electron pulling effect of electronegative fluorine atoms. In PTBF2, two fluorine atoms pull electrons in opposite directions and hence net pulling effect is negligible. As a result, PTBF2 has comparable dipole moment to that of PTB2. In contrast, the very high dipole moment of PTB7 is due to the strong pulling effect of fluorine atom in each thienothiophene unit. Overall, the dipole moments across the isolated oligomers follow the order: $\mu_{PTB2} \approx \mu_{PTBF2} \ll \mu_{PTB7} \approx \mu_{PTBF3}$. This holds equally true for fullerene/oligomer complexes (Figure 8). The dipole moment may control the extent of dissociation of excitons at the donor/acceptor interface. Strong dipole moment facilitates the charge separation, whereas weak dipole moment facilitates charge recombination.

**3.3. Implications to OSC Performance.** The present work is beneficial to the BHJ-based OSC community for two reasons: First, the computed results explain the experimentally observed variable PCE of PTB2, PTB7, PTBF2 and PTBF3 based OSCs. Second, outcomes of the present work highlight the important factors that need be considered while designing the high-performance conjugated polymers of OSCs.

The experimentally reported PCE of OSC is calculated using the equation[51]

$$\eta_e = \frac{V_{oc} J_{sc} FF}{P_{in}} \tag{3}$$

where $V_{oc}$, $J_{sc}$, $P_{in}$, and FF are the open-circuit voltage, the short-circuit current, the incident solar power and the fill factor, respectively. $J_{sc}$ and FF are characteristics of mobilities and lifetimes of charge carriers, and tuning them is complicated.[51,52] Hence, the current focus of OSC research is to increase $V_{oc}$, which is characteristic of the electronic properties of the donor and the acceptor as[53]

$$V_{oc} = \frac{1}{e}[|E_{HOMO}^{Donor}| - |E_{LUMO}^{Acceptor}|] - 0.3V \tag{4}$$

For a given PCBM as an electron acceptor, $V_{oc}$ is approximated by the energy difference between HOMO of conjugated polymer and the LUMO of PCBM, $E_{DA}$. In OSCs, $E_{DA}$ represents the maximum achievable voltage. However, $V_{oc}$ cannot be increased too far by decreasing the HOMO level of a polymer because too low HOMO−HOMO offset hinders hole transport thereby favoring charge recombination. $V_{oc}$ for

PTB7, PTB2, PTBF2, and PTBF3 are 0.74, 0.58, 0.68, and 0.75 V, respectively and the reported PCE of OSCs with these polymers follow the order: PTB7 > PTB2 > PTBF2 > PTBF3.[16] The reason for the superiority of PTB7 against PTB2 can be explained by the higher $V_{oc}$ for PTB7 (higher IP of PTB7 in Figure 4a). However, PTB2 has higher PCE compared to PTBF2 (or PTBF3) despite the fact that PTB2 has lower $V_{oc}$. This may be due to the fact that at the polymer/PCBM interface the electronic structure is more complicated than just the energy levels of these individual materials because of the polarization effect.

The variation of molecular electrostatic potential surfaces (section 3.2.2) and dipole moments (section 3.2.3) across the polymer/fullerene complexes points to the significant contribution of polarization to the induced dipole in the ground state. The charge transfer contribution to the total induced dipole is calculated from the net atomic charges on polymer and fullerene and the polarization contribution is calculated by subtracting the charge transfer component from the total induced dipole. As seen in Table 1, results of different DFT methods (B3LYP, CAM-B3LYP,[54] LC-wPBE,[55] and LC-BLYP[56]) agree that the significant contribution to the interfacial dipole comes from the polarization effect. At the B3LYP level, the polarization contribution to the resulting dipoles of complexes of fullerene with PTB7, PTB2, PTBF2, and PTBF3 are ~95, 75, 74, and 89%, respectively. The present results are in agreement with Linares et al.,[57] in which they found that ~85% of the interfacial dipole at the pentacene/fullerene complex is due to the polarization effect in the ground state.

**Table 1. Polarization Contribution (%) to the Induced Dipole at the Polymer/Fullerene Interface Computed Using Various DFT Functionals Combined with 6-31G(d) Basis Set**

| complex | B3LYP | CAM-B3LYP | LC-BLYP | LC-wPBE |
|---|---|---|---|---|
| PTB7/C60 | 95 | 95 | 95 | 92 |
| PTB2/C60 | 75 | 82 | 87 | 67 |
| PTBF2/C60 | 74 | 82 | 86 | 68 |
| PTBF3/C60 | 89 | 91 | 91 | 87 |

In the excited state, the significant contribution to the interfacial dipole comes from the charge transfer effect. At the B3LYP level, the computed charge transfer contribution to the excited state induced dipole for these complexes range from 65 to 74%. Moreover, the dipole moment of the excited state increases substantially. The change in the interfacial dipole moment ($\Delta\mu_{ge}$) is calculated from the ground state dipole moment ($\mu_g$) and the excited state dipole moment ($\mu_e$) as[50]

$$\Delta\mu_{ge} = [(\mu_{gx} - \mu_{ex})^2 + (\mu_{gy} - \mu_{ey})^2 + (\mu_{gz} - \mu_{ez})^2]^{1/2} \quad (5)$$

The computed values of $\Delta\mu_{ge}$ for complexes of fullerene with PTB7, PTB2, PTBF2, and PTBF3 monomers at the B3LYP level are 23.7, 19.6, 19.2, and 18.9 D, respectively. The values of ~4 and ~16 D are reported for isolated thieno[3,4-*b*]thiophene component in a thienothiophene fluorinated PTB2 monomer[50] and BnDT-DTffBT monomer,[58] respectively. The present results show that $\Delta\mu_{ge}$ increases for polymer/fullerene complex compared to the individual component and PTB7/fullerene has the largest $\Delta\mu_{ge}$ indicating efficient charge separation at the interface. In fact, Zhong et al.[59] have reported that the PCE of P3HT/PCBM device increases with the increase in the molecular dipole moment at the interface.

At the polymer/fullerene interface, frontier molecular orbitals are affected by the interfacial dipole. The energy difference between HOMO levels of polymer and fullerene in the polymer/fullerene complex (also called the HOMO offset ($\Delta_{HOMO}$)) is particularly important parameter because a higher magnitude of $\Delta_{HOMO}$ suggests an efficient hole transfer and hence a charge dissociation at the interface.[57] Values of $\Delta_{HOMO}$ calculated at the B3LYP level for PTB7, PTB2, PTBF2, and PTBF3 are 0.53, 0.50, 0.49, and 0.47 eV, respectively. Although the absolute values of $\Delta_{HOMO}$ in the present calculations suffer from short chain length and the absence of solid-state effect, relative variation of $\Delta_{HOMO}$ for these complexes are consistent with the observed PCE in the order: PTB7 > PTB2 > PTBF2 > PTBF3.

The efficient charge dissociation required for higher quantum yield of OSC could also be explained in terms of the relative free energy difference for charge separation, $\Delta G^{rel}_{CS} = E_S - (IP - EA)$, at the donor/acceptor interface.[60,61] Here, $E_s$ is the singlet excitation energy, IP is ionization potential of the donor and EA is electron affinity of the acceptor. A small $-\Delta G^{rel}_{CS}$ favors recombination loss whereas, a large value of $-\Delta G^{rel}_{CS}$ favors efficient charge dissociation at the donor/acceptor interface.[61] The present calculations at the B3LYP level show that the values of $-\Delta G^{rel}_{CS}$ for PTB7, PTB2, and PTBF2 are 0.47, 0.39, and 0.28 higher, respectively, relative to $-\Delta G^{rel}_{CS}$ (0.38 eV) for PTBF3, again consistent with the observed PCE in the order: PTB7 > PTB2 > PTBF2 > PTBF3.

All of these facts together imply that efficiency of OSC can be increased by designing a conjugated polymer that has low energy gaps, large dipole moment and the proper interfacial energy level offset. In this study, we explored the influence of fluorination on electronic properties. It should be noted that the fluorination may also influence the morphology of the active layer in OSC. The change in the molecular structure of active layer components affects the performance of OSC because of its influence on charge separation and charge carrier mobility as discussed in the recent review.[17] Considering energy gaps and IP, PTB2, and PTB7 have potential for the efficient OSC. However, considering dipole moment and energy level offset, PTB7 is the only promising candidate out of PTB2 derivatives. Hence, the present study supports the experimental findings that only the fluorination of thienothiophene unit of PTB2 increases the PCE of OSC. The present study further suggests that the effort to design efficient conjugated polymers for OSC should be directed not only to pursuing low energy gaps but also to focusing the low IP, low EA, and high interfacial dipole moment.

## 4. CONCLUSIONS

First-principles calculations were employed to investigate the effect of fluorination on electronic properties of isolated polythienothiophene-*co*-benzodithiophenes as well as their complexes with fullerene. Energy gaps ($E^{opt}_g$and $E^{hl}_g$), ionization potentials (IP), electron affinities (EA), dipole moments ($\mu$) and molecular electrostatic potentials (MEP) surfaces of isolated oligomers were computed using ground state (DFT) and excited state (TDDFT) calculations. $E^{opt}_g$ and $E^{hl}_g$ computed for isolated oligomers were extrapolated to the infinite chain limit, which were found to be in good agreement to reported experimental values. The equilibrium separations ($r_{D-A}$), MEP

and $\mu$ for fullerene/polymer complexes were investigated using DFT calculations.

Fluorinated derivatives were found in the present investigation to have increased $E_g^{opt}$, $E_g^{hl}$, IP, EA, and MEP compared to PTB2. The value of $r_{D-A}$ was found to be independent to the fluorine substitution whereas $\mu$ was found to be strongly dependent on fluorine substitution to the thienothiophene units. The relatively smaller energy gaps and stronger dipole moment of PTB7 compared to PTB2 derivatives indicate that PTB7 has more potential to be an efficient electron donor for OSC devices, in agreement with the recent experimental findings. The present study suggests that IP, EA, and interfacial dipole should be given equal attention as energy gaps while further designing the efficient conjugated polymers.

## AUTHOR INFORMATION


### Corresponding Authors

*E-mail: rsb20@uakron.edu.

*E-mail: mtsige@uakron.edu.


### Notes

The authors declare no competing financial interest.

## ACKNOWLEDGMENTS

We are grateful to the National Science Foundation (Grant DMR0847580) for financial support. This work used Kraken and Blacklight computational resources that are provided by the extreme science and engineering discovery environment (XSEDE). The authors thank the University of Akron for additional support.

## REFERENCES


(1) Sariciftci, N. S. Plastic Photovoltaic Devices. *Mater. Today* **2004**, *7*, 36−40.

(2) Hoppe, H.; Sariciftci, N. S. Organic Solar Cells: An Overview. *J. Mater. Res.* **2004**, *19*, 1924−1945.

(3) Brabec, C. J.; Sariciftci, N. S.; Hummelen, J. C. Plastic Solar Cells. *Adv. Funct. Mater.* **2001**, *11*, 15−26.

(4) Darling, S. B.; You, F. The Case for Organic Photovoltaics. *RSC Adv.* **2013**, *3*, 17633−17648.

(5) Bao, Z.; Dodabalapur, A.; Lovinger, A. J. Soluble and Processable Regioregular Poly(3-Hexylthiophene) for Thin Film Field-Effect Transistor Applications with High Mobility. *Appl. Phys. Lett.* **1996**, *69*, 4108−4110.

(6) Krebs, F. C. Fabrication and Processing of Polymer Solar Cells: A Review of Printing and Coating Techniques. *Sol. Energy Mater. Sol. Cells* **2009**, *93*, 394−412.

(7) Raja, M.; Lloyd, G. C. R.; Sedghi, N.; Eccleston, W.; Di Lucrezia, R.; Higgins, S. J. Conduction Processes in Conjugated, Highly Regio-Regular, High Molecular Mass, Poly(3-Hexylthiophene) Thin-Film Transistors. *J. Appl. Phys.* **2002**, *92*, 1441−1445.

(8) Sirringhaus, H.; Brown, P. J.; Friend, R. H.; Nielsen, M. M.; Bechgaard, K.; Langeveld-Voss, B. M. W.; Spiering, A. J. H.; Janssen, R. A. J.; Meijer, E. W.; Herwig, P.; De Leeuw, D. M. Two-Dimensional Charge Transport in Self-Organized, High-Mobility Conjugated Polymers. *Nature* **1999**, *401*, 685−688.

(9) Yue, D.; Khatav, P.; You, F.; Darling, S. B. Deciphering the Uncertainties in Life Cycle Energy and Environmental Analysis of Organic Photovoltaics. *Energy Environ. Sci.* **2012**, *5*, 9163−9172.

(10) He, Z.; Zhong, C.; Su, S.; Xu, M.; Wu, H.; Cao, Y. Enhanced Power-Conversion Efficiency in Polymer Solar Cells Using an Inverted Device Structure. *Nat. Photonics* **2012**, *6*, 593−597.

(11) Skotheim, T. A.; Reynolds, J. *Handbook of Conducting Polymers*; 3rd ed.; CRC Press: Boca Raton, FL, 2007.

(12) Yu, G.; Gao, J.; Hummelen, J. C.; Wudl, F.; Heeger, A. J. Polymer Photovoltaic Cells: Enhanced Efficiencies via a Network of Internal Donor-Acceptor Heterojunctions. *Science* **1995**, *270*, 1789−1791.

(13) Peumans, P.; Yakimov, A.; Forrest, S. R. Small Molecular Weight Organic Thin-film Photodetectors and Solar cells. *J. Appl. Phys.* **2003**, *93*, 3693−3723.

(14) Li, G.; Zhu, R.; Yang, Y. Polymer Solar Cells. *Nat. Photonics* **2012**, *6*, 153−161.

(15) Lee, K. C.; Park, W.; Noh, Y.; Yang, C. Benzodipyrrolidone (BDP)-Based Polymer Semiconductors Containing a Series of Chalcogen Atoms: Comprehensive Investigation of the Effect of Heteroaromatic Blocks on Intrinsic Semiconducting Properties. *ACS Appl. Mater. Interfaces* **2014**, *6*, 4872−4882.

(16) Son, H. J.; Wang, W.; Xu, T.; Liang, Y.; Wu, Y.; Li, G.; Yu, L. Synthesis of Fluorinated Polythienothiophene-co-benzodithiophenes and Effect of Fluorination on the Photovoltaic Properties. *J. Am. Chem. Soc.* **2011**, *133*, 1885−1894.

(17) Chen, W.; Nikiforov, M. P.; Darling, S. B. Morphology Characterization in Organic and Hybrid Solar Cells. *Energy Environ. Sci.* **2012**, *5*, 8045−8074.

(18) Liang, Y.; Xu, Z.; Xia, J.; Tsai, S.; Wu, Y.; Li, G.; Ray, C.; Yu, L. For the Bright Future—Bulk Heterojunction Polymer Solar Cells with Power Conversion Efficiency of 7.4%. *Adv. Mater.* **2010**, *22*, E135−E138.

(19) Liang, Y.; Feng, D.; Wu, Y.; Tsai, S.; Li, G.; Ray, C.; Yu, L. Highly Efficient Solar Cell Polymers Developed via Fine-Tuning of Structural and Electronic Properties. *J. Am. Chem. Soc.* **2009**, *131*, 7792−7799.

(20) Kim, J.; Yun, M. H.; Kim, G.; Lee, J.; Lee, S. M.; Ko, S.; Kim, Y.; Dutta, G. K.; Moon, M.; Park, S. Y.; Kim, D. S.; Kim, J. Y.; Yang, C. Synthesis of PCDTBT-Based Fluorinated Polymers for High Open-Circuit Voltage in Organic Photovoltaics: Towards an Understanding of Relationships between Polymer Energy Levels Engineering and Ideal Morphology Control. *ACS Appl. Mater. Interfaces* **2014**, *6*, 7523−7534.

(21) Kim, B.; Jeong, E. J.; Park, H. J.; Bilby, D.; Guo, L. J.; Kim, J. Effect of Polymer Aggregation on the Open Circuit Voltage in Organic Photovoltaic Cells: Aggregation-Induced Conjugated Polymer Gel and its Application for Preventing Open Circuit Voltage Drop. *ACS Appl. Mater. Interfaces* **2011**, *3*, 674−680.

(22) Alem, S.; Wakim, S.; Lu, J.; Robertson, G.; Ding, J.; Tao, Y. Degradation Mechanism of Benzodithiophene-Based Conjugated Polymers When Exposed to Light in Air. *ACS Appl. Mater. Interfaces* **2012**, *4*, 2993−2998.

(23) Liu, P.; Zhang, K.; Liu, F.; Jin, Y.; Liu, S.; Russell, T. P.; Yip, H.; Huang, F.; Cao, Y. Effect of Fluorine Content in Thienothiophene-Benzodithiophene Copolymers on the Morphology and Performance of Polymer Solar Cells. *Chem. Mater.* **2014**, *26*, 3009−3017.

(24) Iyer, A.; Bjorgaard, J.; Anderson, T.; Kose, M. E. Quinoxaline-Based Semiconducting Polymers: Effect of Fluorination on the Photophysical, Thermal, and Charge Transport Properties. *Macromolecules* **2012**, *45*, 6380−6389.

(25) Wang, N.; Chen, Z.; Wei, W.; Jiang, Z. Fluorinated Benzothiadiazole-Based Conjugated Polymers for High-Performance Polymer Solar Cells without any Processing Additives or Post-treatments. *J. Am. Chem. Soc.* **2013**, *135*, 17060−17068.

(26) Park, J. H.; Jung, E. H.; Jung, J. W.; Jo, W. H. A Fluorinated Phenylene Unit as a Building Block for High-Performance n-Type Semiconducting Polymer. *Adv. Mater.* **2013**, *25*, 2583−2588.

(27) Tumbleston, J. R.; Stuart, A. C.; Gann, E.; You, W.; Ade, H. Fluorinated Polymer Yields High Organic Solar Cell Performance for a Wide Range of Morphologies. *Adv. Funct. Mater.* **2013**, *23*, 3463−3470.

(28) Zhang, Y.; Zou, J.; Cheuh, C.; Yip, H.; Jen, A. K. Significant Improved Performance of Photovoltaic Cells Made from a Partially Fluorinated Cyclopentadithiophene/Benzothiadiazole Conjugated Polymer. *Macromolecules* **2012**, *45*, 5427−5435.

(29) Bhatta, R. S.; Perry, D. S.; Tsige, M. Nanostructures and Electronic Properties of a High-Efficiency Electron-Donating Polymer. *J. Phys. Chem. A* **2013**, *117*, 12628−12634.

(30) Bhatta, R. S.; Tsige, M. Chain Length and Torsional Dependence of Exciton Binding Energies in P3HT and PTB7 Conjugated Polymers: A First Principles Study. *Polymer* **2014**, *55*, 2667−2672.
(31) Becke, A. D. Density-Functional Thermochemistry. III. The Role of Exact Exchange. *J. Chem. Phys.* **1993**, *98*, 5648−5652.
(32) Grimme, S. Semiempirical GGA-Type Density Functional Constructed with a Long-Range Dispersion Correction. *J. Comput. Chem.* **2006**, *27*, 1787−1799.
(33) Bhatta, R. S.; Perry, D. S. Correlated Backbone Torsional Potentials in Poly(3-Methylthiophene). *Comput. Theor. Chem.* **2013**, *1008*, 90−95.
(34) Bhatta, R. S.; Yimer, Y. Y.; Perry, D. S.; Tsige, M. Improved Force Field for Molecular Modeling of Poly(3-Hexylthiophene). *J. Phys. Chem. B* **2013**, *117*, 10035−10045.
(35) Bhatta, R. S.; Yimer, Y. Y.; Tsige, M.; Perry, D. S. Conformations and Torsional Potentials of Poly(3-Hexylthiophene) Oligomers: Density Functional Calculations up to the Dodecamer. *Comput. Theor. Chem.* **2012**, *995*, 36−42.
(36) Darling, S. B. Isolating the Effect of Torsional Defects on Mobility and Band Gap in Conjugated Polymers. *J. Phys. Chem. B* **2008**, *112*, 8891−8895.
(37) Darling, S. B.; Sternberg, M. Importance of Side Chains and Backbone Length in Defect Modeling of Poly(3-Alkylthiophenes). *J. Phys. Chem. B* **2009**, *113*, 6215−6218.
(38) Ling, L.; Lagowski, J. B. DFT Study of Electronic Band Structure of Alternating Triphenylamine-fluorene copolymers. *Polymer* **2013**, *54*, 2535−2543.
(39) Hohenberg, P.; Kohn, W. Inhomogeneous Electron Gas. *Phys. Rev.* **1964**, *136*, B864−B871.
(40) Runge, E.; Gross, E. K. U. Density-Functional Theory for Time-Dependent Systems. *Phys. Rev. Lett.* **1984**, *52*, 997−1000.
(41) Valiev, M.; Bylaska, E. J.; Govind, N.; Kowalski, K.; Straatsma, T. P.; van Dam, H. J. J.; Wang, D.; Nieplocha, J.; Apra, E.; Windus, T. L.; de Jong, W. A. Nwchem: A Comprehensive and Scalable Open-Source Solution for Large Scale Molecular Simulations. *Comput. Phys. Commun.* **2010**, *181*, 1477.
(42) Frisch, M. J.; Trucks, G. W.; Schlegel, H. B.; Scuseria, G. E.; Robb, M. A.; Cheeseman, J. R.; Scalmani, G.; Barone, V.; Mennucci, B.; Petersson, G. A.; Nakatsuji, H.; Caricato, M.; Li, X.; Hratchian, H. P.; Izmaylov, A. F.; Bloino, J.; Zheng, G.; Sonnenberg, J. L.; Hada, M.; Ehara, M.; Toyota, K.; Fukuda, R.; Hasegawa, J.; Ishida, M.; Nakajima, T.; Honda, Y.; Kitao, O.; Nakai, H.; Vreven, T.; Montgomery, J. A., Jr.; Peralta, J. E.; Ogliaro, F.; Bearpark, M.; Heyd, J. J.; Brothers, E.; Kudin, K. N.; Staroverov, V. N.; Kobayashi, R.; Normand, J.; Raghavachari, K.; Rendell, A.; Burant, J. C.; Iyengar, S. S.; Tomasi, J.; Cossi, M.; Rega, N.; Millam, J. M.; Klene, M.; Knox, J. E.; Cross, J. B.; Bakken, V.; Adamo, C.; Jaramillo, J.; Gomperts, R.; Stratmann, R. E.; Yazyev, O.; Austin, A. J.; Cammi, R.; Pomelli, C.; Ochterski, J. W.; Martin, R. L.; Morokuma, K.; Zakrzewski, V. G.; Voth, G. A.; Salvador, P.; Dannenberg, J. J.; Dapprich, S.; Daniels, A. D.; Farkas, O.; Foresman, J. B.; Ortiz, J. V.; Cioslowski, J.; Fox, D. J. *Gaussian 09*, revision A.02; Gaussian, Inc.: Wallingford, CT, 2009.
(43) Kuhn, W. The Absorption Spectrum of Polyenes. *Helv. Chim. Acta* **1948**, *31*, 1780−1799.
(44) Gierschner, J.; Cornil, J.; Egelhaaf, H.-J. Optical Bandgaps of $\pi$-Conjugated Organic Materials at the Polymer Limit: Experiment and Theory. *Adv. Mater.* **2007**, *19*, 173−191.
(45) Cramer, C. J. *Essentials of Computational Chemistry: Theories and Models*, second ed.; John Wiley & Sons: New York, 2004.
(46) Zade, S. S.; Zamoshchik, N.; Bendikov, M. From Short Conjugated Oligomers to Conjugated Polymers. Lessons from Studies on Long Conjugated Oligomers. *Acc. Chem. Res.* **2011**, *44*, 14−24.
(47) Rice, M. J.; Gartstein, Y. N. Theory of Photoinduced Charge Transfer in a Molecularly Doped Conjugated Polymer. *Phys. Rev. B* **1996**, *53*, 10764−10770.
(48) Wu, M. W.; Conwell, E. M. Theory of Photoinduced Charge Transfer in Weakly Coupled Donor-Acceptor Conjugated Polymers: Application to an MEH-PPV:CN-PPV Pair. *Chem. Phys.* **1998**, *227*, 11−17.
(49) Marchiori, C. F. N.; Koehler, M. Dipole Assisted Exciton Dissociation at Conjugated Polymer/Fullerene Photovoltaic Interfaces: A Molecular Study Using Density Functional Theory Calculations. *Synth. Met.* **2010**, *160*, 643−650.
(50) Carsten, B.; Szarko, J. M.; Son, H. J.; Wang, W.; Lu, L.; He, F.; Rolczynski, B. S.; Lou, S. J.; Chen, L. X.; Yu, L. Examining the Effect of the Dipole Moment on Charge Separation in Donor-Acceptor Polymers for Organic Photovoltaic Applications. *J. Am. Chem. Soc.* **2011**, *133*, 20468−20475.
(51) Guo, X.; Zhou, N.; Lou, S. J.; Smith, J.; Tice, D. B.; Hennek, J. W.; Ortiz, R. P.; Navarrete, J. T. L.; Li, S.; Strzalka, J.; Chen, L. X.; Chang, R. P. H.; Facchetti, A.; Marks, T. J. Polymer Solar Cells with Enhanced Fill Factors. *Nat. Photonics* **2013**, *7*, 825−833.
(52) Cheng, Y. C.; Yang, S.; Hsu, C. Synthesis of Conjugated Polymers for Organic Solar Cell Applications. *Chem. Rev.* **2009**, *109*, 5868−5923.
(53) Markus, C.; Scharber, M. C.; Mühlbacher, D.; Koppe, M.; Denk, P.; Waldauf, C.; Heeger, A. J.; Brabec, C. J. Design Rules for Donors in Bulk-Heterojunction Solar Cells—Towards 10% Energy-Conversion Efficiency. *Adv. Mater.* **2006**, *18*, 789−79.
(54) Yanai, T.; Tew, D.; Handy, N. A New Hybrid Exchange-correlation Functional Using the Coulomb-attenuating Method (CAM-B3LYP). *Chem. Phys. Lett.* **2004**, *393*, 51−57.
(55) Vydrov, O. A.; Scuseria, G. E. Assessment of a Long Range Corrected Hybrid Functional. *J. Chem. Phys.* **2006**, *125*, 234109−234118.
(56) Iikura, H.; Tsuneda, T.; Yanai, T.; Hirao, K. Long-range Correction Scheme for Generalized-gradient-approximation Exchange Functionals. *J. Chem. Phys.* **2001**, *115*, 3540−3544.
(57) Linares, M.; Beljonne, D.; Cornil, J.; Lancaster, K.; Bredas, J.; Verlaak, S.; Mityashin, A.; Heremans, P.; Fuchs, A.; Lennartz, C.; Ide, J.; Mereau, R.; Aurel, P.; Ducasse, L.; Castet, F. On the Interface Dipole at the Pentacene-Fullerene Heterojunction: A Theoretical Study. *J. Phys. Chem. C* **2010**, *114*, 3215−3224.
(58) Stuart, A. C.; Tumbleston, J. R.; Zhou, H.; Li, W.; Liu, S.; Ade, H.; You, W. Fluorine Substituents Reduce Charge Recombination and Drive Structure and Morphology Development in Polymer Solar Cells. *J. Am. Chem. Soc.* **2013**, *135*, 1806−1815.
(59) Zhong, Y.; Tada, A.; Geng, Y.; Wei, Q.; Hashimoto, K.; Tajima, K. Donor/Acceptor Interface Modifications in Organic Solar Cells. *J. Photopolym. Sci. Technol.* **2013**, *16*, 181−184.
(60) Liu, T.; Troisi, A. Absolute Rate of Charge Separation and Recombination in a Molecular Model of the P3HT/PCBM Interface. *J. Phys. Chem. C* **2011**, *115*, 2406−2415.
(61) Ohkita, H.; Cook, S.; Astuti, Y.; Duffy, W.; Tierney, S.; Zhang, W.; Heeney, M.; McCulloch, I.; Nelson, J.; Bradley, D. D. C.; Durrant, J. R. Charge Carrier Formation in Polythiophene/Fullerene Blend Films Studied by Transient Absorption Spectroscopy. *J. Am. Chem. Soc.* **2008**, *130*, 3030−3042.